

Electronic Differences between Coordinating Functionalities of Chiral Phosphine–Phosphites and Effects in Catalytic Enantioselective Hydrogenation

Andrés Suárez,[†] Miguel A. Méndez-Rojas,[‡] and Antonio Pizzano^{*,†}

Instituto de Investigaciones Químicas, Consejo Superior de Investigaciones Científicas-Universidad de Sevilla, c/Américo Vespucio s/n, Isla de la Cartuja, 41092 Sevilla, Spain, and Centro de Investigaciones Químicas, Universidad Autónoma del Estado de Hidalgo, Pachuca 42073, Hidalgo, Mexico

Received February 20, 2002

A convenient synthesis of new chiral phosphine–phosphites (P–OP) has been described. The versatility of the synthetic protocol developed has allowed the preparation of ligands with different phosphine fragments and the choice of the stereogenic element location. Analyses of the values of $^1J_{\text{PSe}}$ of the corresponding diselenides are in accord with the expected lower σ -donor ability of the phosphite fragment, with respect to the phosphine group, and with an increase of phosphine basicity after substitution of phenyl substituents by methyl groups. Inspection of $\nu(\text{CO})$ values on a series of complexes $\text{RhCl}(\text{CO})(\text{P–OP})$ demonstrated a variable π -acceptor ability of the phosphite group, compensating for the change of basicity of the phosphine functionality, as well as having a rather reduced electron density at the metal center compared with diphosphine analogues. The distinct nature of the phosphorus functionalities has also been evidenced in rhodium-catalyzed enantioselective hydrogenation of methyl *Z*- α -acetamido-cinnamate (MAC). Thus, the coordination mode of the substrate is governed by the chiral ligand, directing the olefinic bond to a *cis* position with respect to the phosphite group, as demonstrated by NMR studies performed with $[\text{Rh}(\text{P–OP})(\text{MAC})]^+$ complexes. In consequence, the phosphite group has a greater impact on the enantioselectivity of the product. However, the optical purity of the process also depends on the nature of the phosphine group, and hence, an appropriate election of both phosphorus functionalities is required for the attainment of excellent enantioselectivities (99% ee).

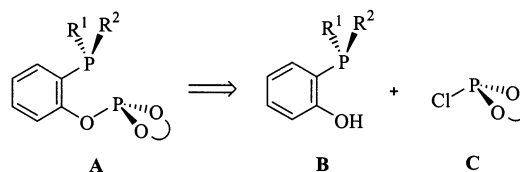
Introduction

Chelating ligands with two different coordinating functionalities (L–L') are receiving a growing interest in asymmetric catalysis.¹ When compared with broadly used C_2 symmetric derivatives (L–L), the former can introduce a bigger number of diastereomeric transition states making the stereocontrol of the process more difficult.² However, this complicated picture can be greatly simplified if the bidentate ligand influences the coordination mode of the prochiral substrate, dictating the coordination position where the stereogenic center will be generated.³ Therefore, the bigger complexity introduced by C_1 symmetric ligands should be advantageous, since they offer the possibility of optimizing fragments L and L', thus rendering chiral environments inaccessible for C_2 symmetric ligands.

With respect to processes catalyzed by medium- and late-transition metals, the large diversity of bifunctional

ligands of the type P–N, P–O, P–P', or P–S has been applied in different transformations.⁴ In particular, we have been interested in the synthesis of chiral phosphine–phosphites and their application in asymmetric catalysis. More interestingly, ligands of this kind have produced a benchmark in the study of asymmetric hydroformylation reactions giving outstanding enantioselectivities associated with a remarkable substrate scope.⁵ These bifunctional molecules once again deserve attention and have provided satisfactory results in several asymmetric catalytic processes such as hydrogenation and allylic substitution.⁶

In this contribution we report the synthesis of new phosphine–phosphites based on a rather rigid achiral *o*-oxyphenyl bridge (A).⁷ The synthetic protocol de-



scribed herein allows the preparation of a series of ligands which can differ in the nature of the phosphine fragment, as well as in the position of the stereogenic element(s), covering a wide structural diversity for catalyst optimization.⁸ In addition, we have performed

* To whom correspondence should be addressed. E-mail: pizzano@cica.es.

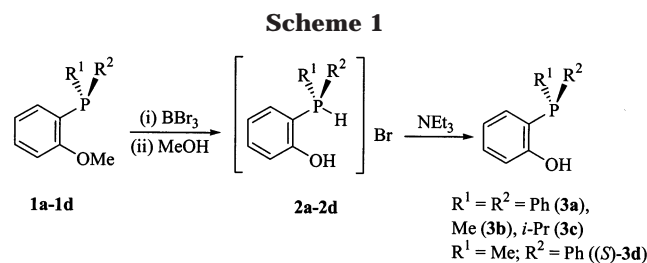
[†] Instituto de Investigaciones Químicas.

[‡] Centro de Investigaciones Químicas.

(1) *Comprehensive Asymmetric Catalysis*; Jacobsen, E. N., Pfaltz, A., Yamamoto, H., Eds; Springer, Berlin, Germany, 1999.

(2) Whitesell, J. K. *Chem. Rev.* **1989**, *89*, 1581.

(3) For successful applications of this concept see: (a) Evans, D. A.; Campos, K. R.; Tedrow, J. S.; Michael, F. E.; Cagne, M. R. *J. Am. Chem. Soc.* **2000**, *122*, 7905. (b) Prétot, R.; Pfaltz, A. *Angew. Chem., Int. Ed.* **1998**, *37*, 323.



studies regarding the electronic characteristics of these ligands and about their performance in rhodium-catalyzed olefin asymmetric hydrogenation. These results have been complemented by information about ligand structure, determined by an X-ray crystallography study, as well as with NMR investigations regarding the coordination mode of the prochiral olefin toward the metal–ligand moiety.

Results and Discussion

Ligand Synthesis. We initially pursued a versatile synthesis of phosphine–phosphites of type **A** that can allow us their application in asymmetric catalysis following a modular approach. As shown below, we have approached the synthesis of phosphine–phosphites **A** by the condensation of the appropriate phenol–phosphine **B**^{9,10} and chlorophosphite **C**. Reagents **B** can be conveniently obtained by demethylation of *o*-anisyl phosphines with BBr_3 .¹¹ Thus, treatment of phosphine **1a** (Scheme 1) with 2.3 molar equiv of BBr_3 , followed by reaction with MeOH, produced the phosphonium bromide **2a**. This reaction sequence also cleanly yielded the corresponding methyl (**2b**) and isopropyl (**2c**) derivatives.

(4) See for instance; P–N ligands: Alcock, N.; Hulmes, D. I.; Brown, J. M. *J. Chem. Soc., Chem. Commun.* **1995**, 395. Wimmer, P.; Wildham, M. *Tetrahedron: Asymmetry* **1995**, 6, 657. P–O ligands: Nandy, M.; Jin, J.; RajanBabu, T. V. *J. Am. Chem. Soc.* **1999**, 121, 9899. Uozumi, Y.; Tanahashi, A.; Lee, S.-Y.; Hayashi, T. *J. Org. Chem.* **1993**, 58, 1945. P–S ligands: Hauptman, E.; Fagan, P. J.; Marshall, W. *Organometallics* **1999**, 18, 2061. P–P' ligands: Ireland, T.; Grossheimann, G.; Wieser-Jeunesse, C.; Knochel, P. *Angew. Chem., Int. Ed.* **1999**, 38, 3212. Ohashi, A.; Imamoto, T. *Tetrahedron Lett.* **2001**, 42, 1099. Tanaka, K.; Fu, G. C. *J. Org. Chem.* **2001**, 66, 8177.

(5) (a) Nozaki, K.; Sakai, N.; Nanno, T.; Higashijima, T.; Mano, S.; Horiuchi, T.; Takaya, H. *J. Am. Chem. Soc.* **1997**, 119, 4413. (b) Horiuchi, T.; Ohta, T.; Shirakawa, E.; Nozaki, K.; Takaya, H. *J. Org. Chem.* **1997**, 62, 4285.

(6) (a) Deerenberg, S.; Schrekker, H. S.; Strijdonck, G. P. F.; Kamer, P. C. J.; van Leeuwen, P. W. N. M. *J. Org. Chem.* **2000**, 65, 4810. (b) Deerenberg, S.; Kamer, P. C. J.; van Leeuwen, P. W. N. M. *Organometallics* **2000**, 19, 2065. (c) Deerenberg, S.; Pàmies, O.; Diéguez, M.; Claver, C.; Kamer, P. C. J.; van Leeuwen, P. W. N. M. *J. Org. Chem.* **2001**, 66, 7626. (d) Pàmies, O.; Diéguez, M.; Net, G.; Ruiz, A.; Claver, C. *J. Org. Chem.* **2001**, 66, 8364.

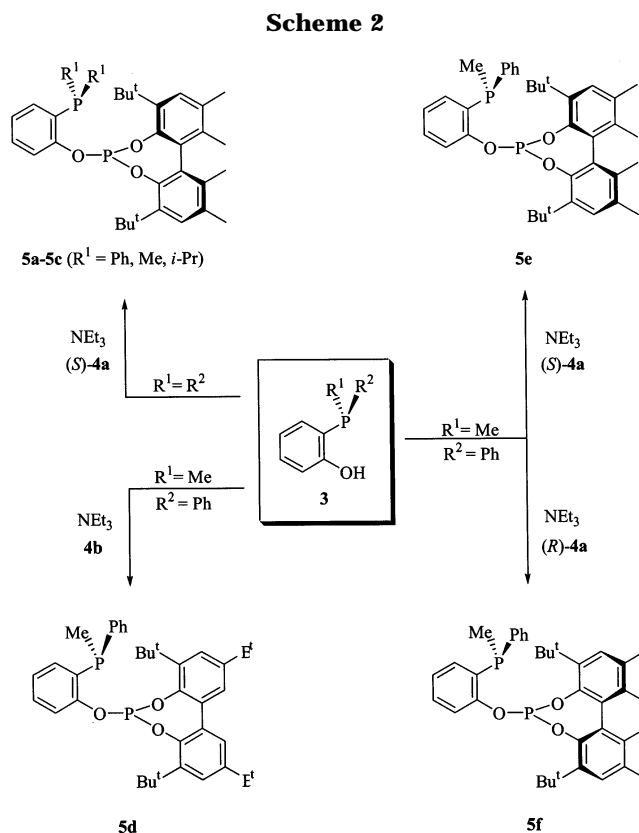
(7) For other derivatives based on this backbone see: (a) Baker, M. J.; Pringle, P. *J. Chem. Soc., Chem. Commun.* **1993**, 314. (b) Kranich, R.; Eis, K.; Geis, O.; Mühle, S.; Bats, J. W.; Schmalz, H.-G. *Chem. Eur. J.* **2000**, 6, 2874.

(8) This synthetic protocol has been described in a preliminary form: Suárez, A.; Pizzano, A. *Tetrahedron: Asymmetry* **2001**, 12, 2501.

(9) Several methods have been used for the synthesis of diverse phenol phosphines. For representative procedures see: (a) Rauchfuss, T. B. *Inorg. Chem.* **1977**, 16, 2966. (b) Heinicke, J.; Kadyrov, R.; Kindermann, M. K.; Koesling, M.; Jones, P. G. *Chem. Ber.* **1996**, 129, 1547. (c) Schmutzler, R.; Schomburg, D.; Bartsch, R.; Stelzer, O. *Z. Naturforsch.* **1984**, 39, 1177.

(10) Only recently, Jugé and co-workers have described the first enantioselective synthesis of a *P*-stereogenic 2-hydroxyaryl phosphine ((*R*)-*o*-anisyl-2-hydroxynaphthylphenyl phosphine) using an alternative procedure; however, this method requires difficultly accessible enantiopure phosphinite boranes: Moulin, D.; Bago, S.; Bauduin, C.; Darcel, C.; Jugé, S. *Tetrahedron: Asymmetry* **2000**, 11, 3939.

(11) This sequence of reactions has been used previously in the synthesis of some quinolyl phosphines: Sembiring, S. B.; Colbran, S. B.; Craig, D. C. *Inorg. Chem.* **1995**, 34, 761.



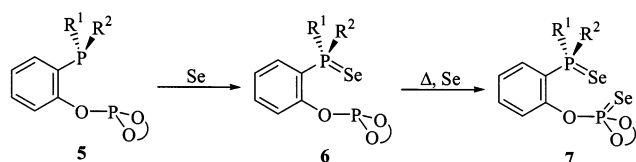
Subsequent treatment of phosphonium salts **2a–c** with NEt_3 produced a quantitative deprotonation to afford the corresponding phenol–phosphines **3**. However, the intermediacy of the phosphonium salts is of practical convenience, since alkyl derivatives **2b** and **2c** are less air-sensitive solids than their phosphine counterparts. For this reason we have used them as stock reagents to generate in situ the corresponding phosphines.

A touchstone to the procedure depicted in Scheme 1 comes from the investigation of the reaction sequence on an enantiopure starting material. Noteworthy, treatment of (*S*)-PAMP¹² produced the corresponding phenol–phosphine (*S*)-**3d** without racemization. This was confirmed by a comparative analysis, performed by ³¹P{¹H} NMR spectroscopy, of the phosphine–phosphites obtained by condensation between (*S*)-**3d** and (*rac*)-**3d** with chlorophosphite (*S*)-**4a** (see Experimental Section). The expected retention of phosphorus configuration was ensured by the preparation of the borane adduct of (*S*)-**3d**,¹⁰ previously described in the literature, and examination of its optical rotation.

Finally, a simple condensation between phenol phosphines **3** and an appropriate chlorophosphite **4** led to the desired phosphine–phosphites in good yields (**5**, Scheme 2). For this purpose we intentionally chose both enantiomers of 3,3'-di-*tert*-butyl-5,5',6,6'-tetramethyl-2,2'-bisphenoxyphosphorus chloride (**4a**),¹³ as well as conformationally flexible 3,3',5,5'-tetra-*tert*-butyl-2,2'-bisphenoxyphosphorus chloride (**4b**),¹⁴ to cover a variety of situations with respect to the position of the chiral element(s) in the ligand: at the phosphite, at the phosphine, or at both fragments.

(12) Jugé, S.; Stéphan, M.; Laffitte, J. A.; Genet, J. P. *Tetrahedron Lett.* **1990**, 31, 6357.

Scheme 3



Electronic Characteristics of Ligands 5. The most interesting feature of molecules **5** is the presence of two phosphorus functionalities with rather different electronic properties. When coordinated to a metal center, a good σ -donor ability can be expected for the phosphine group, whereas a phosphite fragment should be a poorer σ -donor and a better π -acceptor. A simple way of evaluating the σ -donor ability of either a phosphine or a phosphite functionality is by measuring the magnitude of $^1J_{\text{SeP}}$ in the ^{77}Se isotopomer of the corresponding phosphine–selenide or seleno–phosphate, respectively.¹⁵ To estimate the donor abilities of both phosphorus functionalities in compounds **5** we prepared the corresponding diselenides **7** by simply reacting phosphine–phosphites **5** with elemental selenium in toluene at 100 °C (Scheme 3). Interestingly, this reaction proceeded in a stepwise manner through the intermediacy of phosphine selenides **6**, and while the phosphine fragment showed high reactivity (for instance $t_{1/2}$ is ca. 0.5 h at room temperature for **5b**, Figure 1), the phosphite functionality was rather unreactive, needing prolonged heating times (2–8 days) to complete the reaction. Values of ^{31}P – ^{77}Se coupling constants observed in compounds **7** (CDCl_3) are compiled in Table 1.

From the magnitude of $^1J_{\text{PSe}}$ in compounds **7** it is possible to draw some interesting conclusions. First, the phosphine fragments of ligands **5** exhibit the expected donor ability trend, and are ordered on a decreasing basicity (including in parentheses the coupling constant in Hz of the phosphine–selenide fragment of **7**, entries 1–2 and 4–6) as follows: **5b** (703) > **5d** (716), **5e** (711), **5f** (716) > **5a** (732),¹⁵ i.e., by successive substitution of methyl by phenyl groups. It should also be noticed that the value obtained for the isopropyl derivative **7c** (719 Hz, entry 3) is higher than expected, since this ligand should be the more basic at the phosphine site.¹⁶

On the other hand, the selenophosphate fragment of compounds **7** showed, as expected, a markedly higher value of $^1J_{\text{PSe}}$ than the phosphine–selenide functionality. All compounds exhibited coupling constants in the range 1053–1061 Hz, therefore there are no significant differences between them, although they are clearly higher (ca. 30–40 Hz) than values exhibited by acyclic triaryl phosphites.^{15c} This further reduced basicity can

(13) The two enantiomers of chlorophosphite **4a** can be readily prepared from the corresponding optically active bisphenol. These diols are easily available on multigram scale, see: Alexander, J.; Schrock, R. R.; Davis, W. M.; Hultsch, K. C.; Hoveyda, A. H.; Houser, J. H. *Organometallics* **2000**, *19*, 3700.

(14) Buisman, G. J. H.; Kamer, P. C. J.; van Leeuwen, P. W. N. M. *Tetrahedron: Asymmetry* **1993**, *4*, 1625.

(15) (a) Allen, D. W.; Taylor, B. F. *J. Chem. Soc., Dalton Trans.* **1982**, 51. (b) Socol, S. M.; Verkade, J. G. *Inorg. Chem.* **1984**, *23*, 3487. (c) Barnard, T. S.; Mason, M. R. *Organometallics* **2001**, *20*, 206.

(16) We do not have a definite explanation for this deviation. However, it could be due to a distortion of the molecule caused by steric hindrance. In this respect it can be recalled that highly basic $\text{Bu}^t_3\text{P}=\text{Se}$ also exhibited a lower coupling constant value than expected (712 Hz, ref 15).

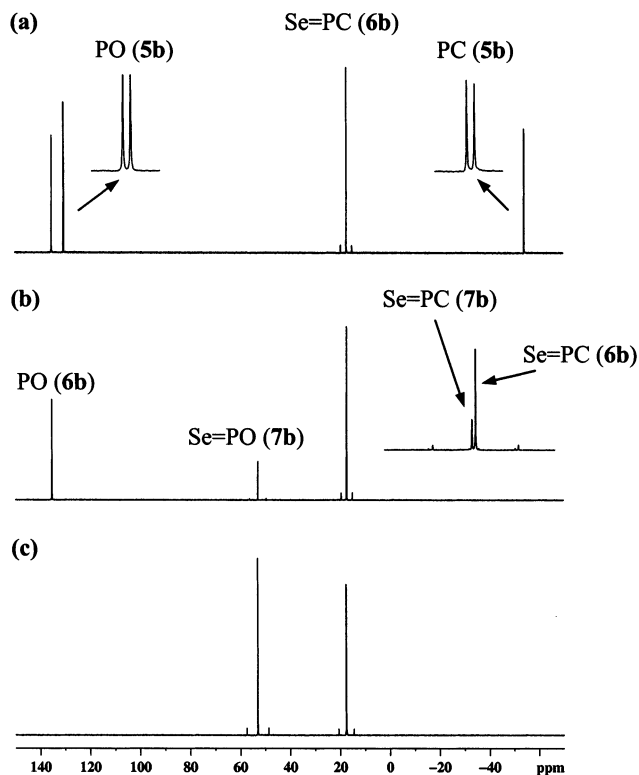
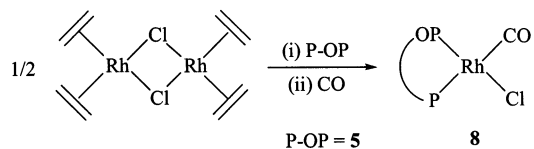


Figure 1. $^{31}\text{P}\{^1\text{H}\}$ NMR ($\text{C}_6\text{D}_5\text{CD}_3$, 162 MHz) of the reaction between **5b** and Se: (a) 30 min, room temperature; (b) 18 h, 100 °C; and (c) 3 d, 100 °C.

Table 1. ^{31}P – ^{77}Se Coupling Constants (Hz) in Compounds **7**

entry	compd	$^1J_{\text{PSe}}(\text{phosphine})$	$^1J_{\text{PSe}}(\text{phosphite})$
1	7a	732	1058
2	7b	703	1053
3	7c	719	1053
4	7d	716	1053
5	7e	711	1061
6	7f	716	1055

Scheme 4



be attributed to the geometrical constraint produced by the cyclic nature of the phosphite fragment.¹⁷

To ascertain the electronic properties of ligands **5** we have prepared a series of compounds $\text{RhCl}(\text{CO})(\mathbf{5})$,¹⁸ as summarized in Scheme 4. The resulting complexes **8** exhibit spectroscopic data in accord with the proposed formulation. The low value of the coupling constant $^1J_{\text{PRh}}$ exhibited by the phosphine fragment (ca. 120 Hz) is indicative of a trans coordination between this functionality and the CO ligand,¹⁹ further confirmed by an X-ray study (see below).

All compounds **8** exhibit very similar $\nu(\text{CO})$ values, in the proximity of 2050 cm^{-1} . These are higher by ca.

(17) Kroshefsky, R. D.; Verkade, J. G. *Inorg. Chem.* **1979**, *18*, 469.

(18) The magnitude of this parameter has been amply used as a measure of the electron density at a metal center; for a recent application see: Serron, S.; Huang, J.; Nolan, S. P. *Organometallics* **1998**, *17*, 534.

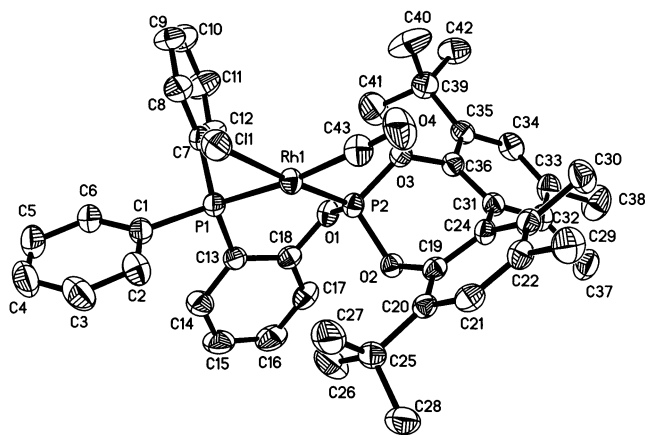


Figure 2. ORTEP drawing of **8a** with the atom-labeling scheme. Thermal ellipsoids are drawn at the 30% probability level (hydrogen atoms and solvent molecule are omitted for simplicity).

Table 2. Selected Bond Lengths (Å) and Angles (deg) for **8c**

C(43)–Rh(1)	1.902(5)
Cl(1)–Rh(1)	2.3651(12)
P(1)–Rh(1)	2.3234(12)
P(2)–Rh(1)	2.1484(12)
P(2)–Rh(1)–P(1)	88.58(4)
C(43)–Rh(1)–Cl(1)	89.02(15)
P(2)–Rh(1)–Cl(1)	176.25(5)
P(1)–Rh(1)–Cl(1)	91.73(4)

50 cm⁻¹ than those reported for the diphosphine analogues RhCl(CO)(R₂PCH₂CH₂PR₂),^{20,21} clearly indicating that ligands **5** give rise to less electron-rich compounds than the chiral diphosphines most often used in asymmetric catalysis.

Structure of Coordinated Phosphine–Phosphites. To obtain information about the structure of a coordinated phosphine–phosphite **5** we have studied by X-ray crystallography compound **8a**. Figure 2 shows an ORTEP view of the molecular structure of the complex, while Table 2 collects the values of some selected bond distances and angles. This complex shows square-planar coordination, with the carbonyl trans to the phosphine fragment. A clear difference between the distances of Rh–P bonds, that corresponding to the phosphite being shorter, is observed (2.15 vs 2.32 Å). A similar observation has been described for other phosphine–phosphite derivatives. Also notably, the rigidity of the backbone caused by the 1,2-phenylene ring imposes a rather small bite angle (ca. 89°) compared with values obtained with a phosphine–phosphite with an aliphatic bridge (ca. 97°)^{6a} or with BINAPHOS (ca. 96°).²²

Most noteworthy is the structure of the coordinated phosphine–phosphite. Thus, the phosphite fragment is

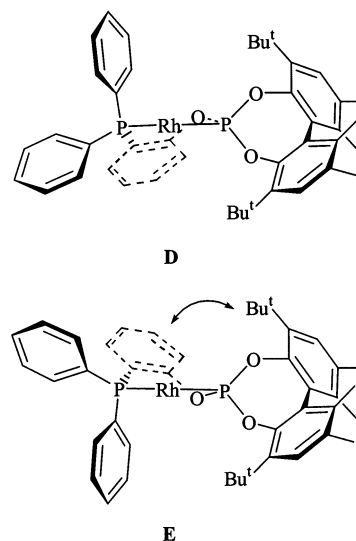
(19) The magnitude of $^1J_{\text{PRh}}$ has been widely used as a structural tool in the analysis of rhodium complexes. The magnitude of this parameter depends markedly on the ligand situated in the trans position with respect to the phosphine/phosphite ligand, being larger for a phosphorus trans to chloride than to a carbonyl ligand. See for instance: Naaktgeboren, A. J.; Nolte, R. J. M.; Drenth, W. *J. Am. Chem. Soc.* **1980**, *102*, 3350.

(20) Sanger, A. R. *J. Chem. Soc., Dalton Trans.* **1977**, 121.

(21) Del Zotto, A.; Costella, L.; Mezzetti, A.; Rigo, P. *J. Organomet. Chem.* **1991**, *414*, 109.

(22) Nozaki, K.; Sato, N.; Tomomura, Y.; Yasutomi, M.; Takaya, H.; Hiya, T.; Matsubara, T.; Koga, N. *J. Am. Chem. Soc.* **1997**, *119*, 12779.

roughly divided in two halves by the coordination plane. This causes one Bu^t group to be placed below the coordination plane toward the CO ligand, and the other above the plane directed to the backbone. The conformation of the latter, with the phenylene group oriented down the coordination plane, is similar to that observed in other related complexes.^{7b,23} This arrangement should minimize the interaction between the backbone and the phosphite moiety (structure **D**), whereas the alternative conformation with the backbone aromatic ring placed above the coordination plane would be hampered by its proximity to the upper Bu^t group (**E**). As a consequence



of the backbone conformation, a chiral, propeller-like²⁴ distribution of the phenyl groups of the phosphine fragment is produced, such that the substituent defined by C(7) occupies an edge-oriented, pseudoaxial position, while the phenyl defined by C(1) is placed in a pseudo-equatorial position with a face orientation.

In good agreement with the assumption of a preferred conformation, a 2D ¹H–¹H NOESY experiment performed with compound **8c** showed an intense NOE cross-peak between the aromatic proton placed ortho with respect to the phosphine group and only one of the methine protons of the Prⁱ groups (Figure 3). In addition, ³¹P{¹H} NMR studies performed at variable temperature with the latter compound displayed the existence of only one species in solution in the range of 300–180 K.

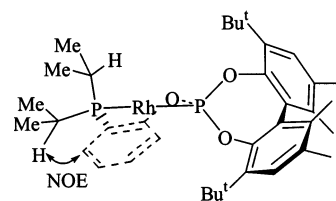
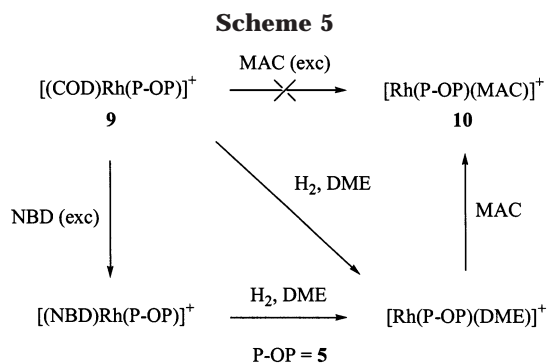


Figure 3.

Behavior of Ligands **5** in the Asymmetric Hydrogenation of Methyl *Z*-α-acetamido-cinnamate.

(23) Sembring, S. B.; Colbran, S. B.; Craig, D. C.; Sander, M. L. *J. Chem. Soc., Dalton Trans.* **1995**, 3731.

(24) This distribution is observed in a great number of bis aryl phosphines with a chiral backbone, see for instance: Noyori, R. *Asymmetric Catalysis in Organic Synthesis*, John Wiley and Sons: New York, 1994.



(a) Structure of $[\text{Rh}(5)(\text{MAC})]^+$ Complexes. We have next examined the coordination mode of methyl *Z*- α -acetamidocinnamate (MAC) in compounds of composition $[\text{Rh}(\text{P}-\text{OP})(\text{MAC})]^+$. To prepare the enamide adducts, we first synthesized compounds of composition $[(\text{COD})\text{Rh}(\text{P}-\text{OP})]\text{BF}_4$ (**9**). These complexes were simply obtained by addition of a stoichiometric amount of ligand **5** to complex $[(\text{COD})_2\text{Rh}]\text{BF}_4$. All compounds **9** showed at room temperature NMR spectra composed of one set of resonances. To investigate the possible importance of dynamic processes such as backbone mobility, we additionally studied compounds **9a** and **9d** by $^{31}\text{P}\{^1\text{H}\}$ NMR spectroscopy in the 298–180 K temperature range. The former exhibited in the entire temperature interval the existence of only one compound in solution. Note that this observation parallels the behavior exhibited by **8c**, and evinces the rigidity of the coordinated phosphine–phosphite. In contrast, compound **9d** displayed a fluxional character, and while at 298 K it showed two doublet doublets, lowering the temperature produced a broadening of both resonances, each of which coalesced at 230 K, and finally split at lower temperatures to give two doublet doublets indicative of two species in solution. The difference in behavior between **9a** and **9d** should be a consequence of the flexible phosphite fragment existing in the latter compound, and therefore, the dynamic behavior of **9d** can be ascribed to the interconversion between the corresponding atropisomers,²⁵ which in view of the interaction between the phenylene bridge and the phosphite moiety mentioned above will probably be accompanied by a backbone conformational change.

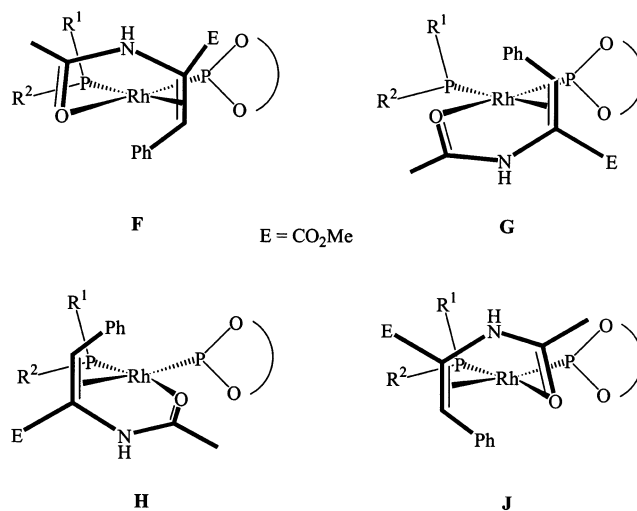
We initially attempted the generation of MAC adducts by the direct reaction between $[(\text{COD})\text{Rh}(5\text{a})]\text{BF}_4$ and the enamide (Scheme 5). Interestingly, no interaction was observed between this compound and a large excess of the enamide (ca. 100 molar equiv) after 3 d at room temperature. As an alternative, we also studied the hydrogenation of compound **9a**. Thus, exposure of a solution of **9a** in 1,2-dimethoxyethane (DME) to 4 atm of hydrogen produced the apparition of a new compound characterized in the $^{31}\text{P}\{^1\text{H}\}$ NMR by two doublet doublets at δ 135.4 ($^1J_{\text{RhP}} = 348$ Hz, $^2J_{\text{PP}} = 90$ Hz) and δ 37.4 ($^1J_{\text{RhP}} = 189$ Hz), along with minor impurities.²⁶ The main species showed the characteristic signals of

(25) Suárez, A.; Pizzano, A.; Fernández, I.; Khiar, N. *Tetrahedron: Asymmetry* **2001**, *12*, 633.

(26) We have noted a rather low reactivity of **9a** toward hydrogen compared with diphosphine-based catalyst precursors. This observation is in good agreement with the behavior described for other phosphine–phosphite derivatives (ref 6d) and could be ascribed to the rather low donating ability of ligands **5**.

the phosphine–phosphite ligand in the ^1H NMR spectrum as well as broad resonances attributable to coordinated DME. Subsequent addition of 1 equiv of MAC produced the corresponding complex $[\text{Rh}(5\text{a})(\text{MAC})]^+$ (**10a**), along with minimal amounts of the starting material and other unidentified species. However, for a cleaner generation of **10a** it is more convenient to start with norbornadiene derivative $[(\text{NBD})\text{Rh}(5\text{a})]\text{BF}_4$.²⁷ Following this sequence of reactions we also prepared the isopropyl derivative $[\text{Rh}(5\text{c})(\text{MAC})]^+$ (**10c**).

Considering the C_1 symmetric nature of ligands **5** there are four possible diastereomers of composition $[\text{Rh}(\text{P}-\text{OP})(\text{MAC})]^+$: two with the olefin cis to the phosphite (structures **F** and **G**) and two cis to the phosphine (**H** and **J**). We have initially investigated the



coordination mode of the enamide ligand by analyzing in more detail the structures of compounds **10** by means of complementary NMR experiments. Thus, the 2D $^{31}\text{P}-^1\text{H}$ correlation experiment showed a coupling between the olefinic proton (assigned in turn by a 2D $^{13}\text{C}-^1\text{H}$ correlation experiment) and the phosphorus of the phosphite, but not with that of the phosphine (Figure 4). This can be compared with the analogue complex containing diphosphine BisP*, studied by Gridnev and Imamoto.²⁸ In the latter case, the corresponding proton couples only with the phosphorus nucleus cis to the olefin group. In the particular case of compound **10c**, coupling constants $^3J_{\text{HP}} = 4.8$ Hz and $^2J_{\text{HRh}} = 2.8$ Hz could be obtained by comparison of the ^1H NMR spectrum with the phosphorus selectively decoupled experiments. These values are practically identical with those observed in the mentioned BisP* derivative. In

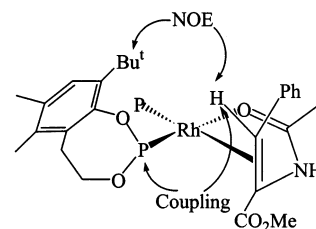


Figure 4.

(27) Borner, A.; Heller, D. *Tetrahedron Lett.* **2001**, *42*, 223.

(28) Gridnev, I. D.; Higashi, N.; Asakura, K.; Imamoto, T. *J. Am. Chem. Soc.* **2000**, *122*, 7183.

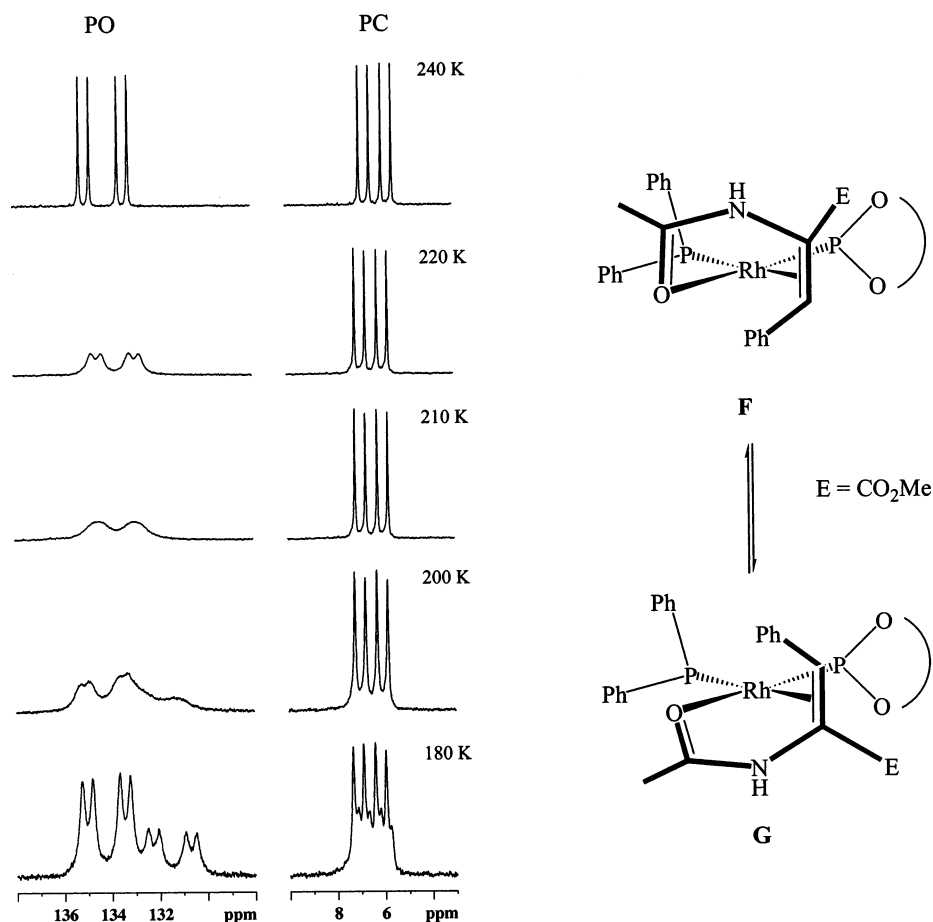


Figure 5. $^{31}\text{P}\{^1\text{H}\}$ NMR (CD_2Cl_2 , 162 MHz) variable-temperature spectra of **10a**.

addition, compounds **10a** and **10c** showed intense NOE cross-peaks in the 2D ^1H - ^1H NOESY experiment between the olefinic proton and the lower field Bu^t group. Overall, these data strongly support structures **F** and **G**, which possess the olefin group coordinated cis with respect to the phosphite, for compounds **10**.²⁹

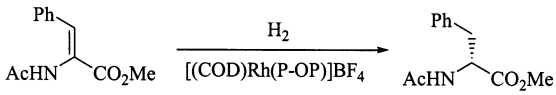
Multinuclear NMR spectra obtained with compounds **10** indicated the existence in solution of one set of resonances according to either the presence of one compound or a fast interchange between several species in the NMR scale time. To discriminate between these possibilities we next examined compounds **10** by variable-temperature $^{31}\text{P}\{^1\text{H}\}$ NMR. Thus, compound **10a** showed one sharp set of signals from room temperature to 240 K (Figure 5). If additionally cooled, the phosphite signal broadened, coalesced at 210 K, and finally split into two doublet doublets with approximately 2:1 relative intensity. In turn, the phosphine signal only broadened slightly and the presence of the minor species was only detected at 180 K, as a doublet doublet overlapped with the resonance corresponding to the major species. In the case of **10c** coalescence was observed at 200 K, while at the lowest temperature investigated (180 K) it was not reached in the slow exchange regime. As in the former case, broadening was much higher in the phosphite signal. Taking into consideration the similarity in chemical shift and coupling constants between the two species in the low exchange spectrum, it is reasonable to assume that both

compounds have the MAC molecule in the same coordination mode (i.e. olefin cis to the phosphite). Then, two distinct possibilities can be considered for the dynamic behavior observed: (i) exchange between **F** and **G** diastereomers differing in the olefin coordinated face and (ii) interchange between conformers which differ in their backbone structure. An estimation of ca. 9 kcal mol⁻¹ for the activation barrier of the dynamic process observed in **10a** coincides with that obtained for the intramolecular olefin face exchange in similar compounds.^{28,30} From these data, as well from the conformational preference observed in **8c** and **9a**, we incline toward the first possibility to explain the dynamic behavior exhibited by compounds **10**.

(b) Performance of Ligands 5 in the Asymmetric Hydrogenation of MAC. Taking advantage of our ligand design, which enables us to choose the position of the stereogenic element of the ligand, we next analyzed the performance of ligands **5** in MAC asymmetric hydrogenation (Table 3). From the coordination mode described above, a higher influence of the phosphite fragment on the enantioselectivity of the process can be expected. Indeed, the configuration of the bi-phenyl moiety controls the enantiomer produced. Thus, catalyst precursor **9a** with *S* configuration at the phosphite produced the *R* enantiomer of the product, while **9f** produced the opposite, both with excellent ee values (99%). These results are in good accord with a recent revisitation of the quadrant rule, since an *S*

(29) Recently, Claver and van Leeuwen have proposed the same coordination mode for a derivative of a phosphine-phosphite: ref **6c**.

(30) Kadyrov, R.; Freier, T.; Heller, D.; Michalik, M.; Selke, R. *Chem. Commun.* **1995**, 1745.

Table 3. Results of the Asymmetric Hydrogenations^a


entry	cat. precursor	conversion	% ee (conf)
1	9a	100	99.5 (<i>R</i>)
2	9b	100	56.1 (<i>R</i>)
3	9c	20	90.6 (<i>R</i>)
4	9d	45	22.0 (<i>S</i>)
5	9e	90	70.3 (<i>R</i>)
6	9f	100	99.0 (<i>S</i>)

^a Reactions were carried out at room temperature under an initial H₂ pressure of 4 atm and 0.2 M dichloromethane solutions of substrate, using the appropriate catalyst precursor for 16 h (entries 1–3) or 24 h (entries 4–6). Conversion was determined by ¹H NMR and ee by chiral GC.

phosphite would be expected to exert the higher steric impediment in the lower right quadrant.²⁸ Then, the result obtained with catalyst precursor **9d** can be ascribed to the coexistence of species with the two configurations of the phosphite fragment,³¹ since the conformational flexibility of this group has been observed in the catalyst precursor. Interestingly, this dynamic process can be responsible for the lower activity displayed by catalyst originating from **9d**. Thus, taken as a reference a ligand with *S* configuration, a change of configuration of the phosphite fragment in species **F** would lead to a less reactive **F'** derivative (Figure 6).³² Otherwise the low activity displayed by the isopropyl derivative **9c** can be simply attributed to the steric encumbrance imposed by the PPr₂ group.³³

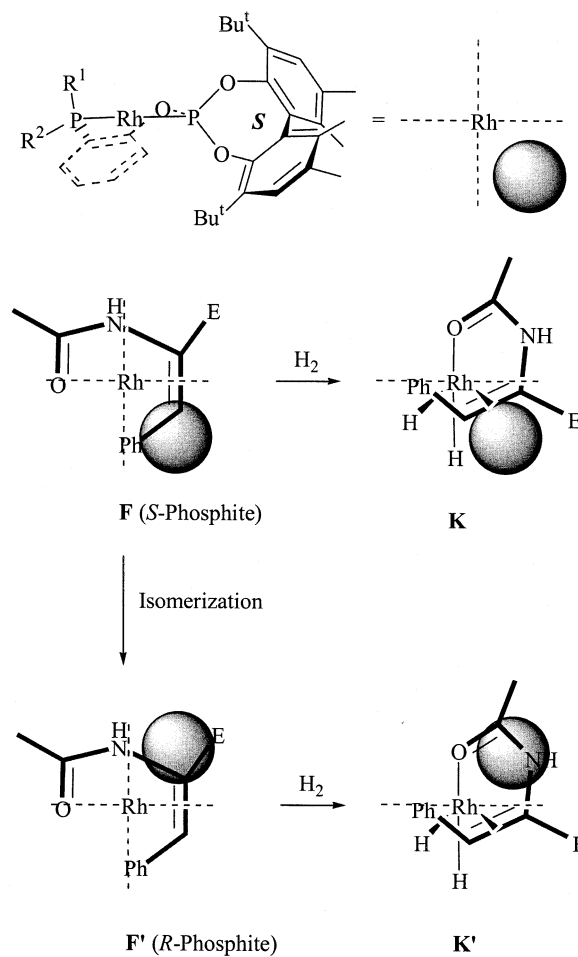
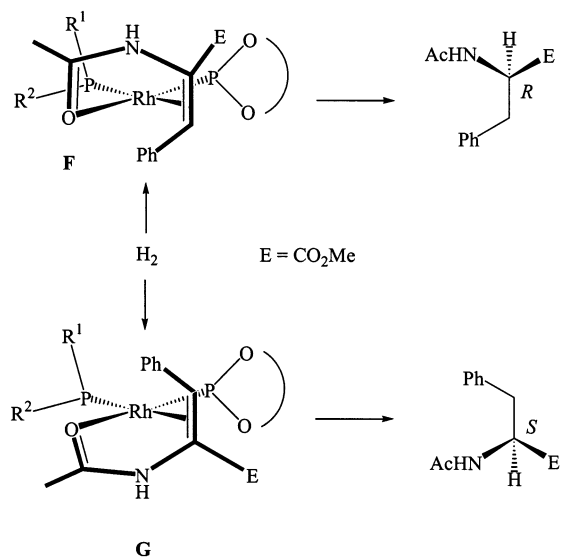
The achievement of a high enantioselectivity needs, in addition, an appropriate phosphine group. Derivatives **9a**, **9c**, and **9f** achieved good to excellent enantioselectivities (90–99% ee), while compounds **9b** and **9e** produced lower optical purities (56 and 70% ee, respectively). Although at the actual level of understanding of this catalytic system it is difficult to give a definite explanation for this secondary ligand influence, a reasonable interpretation can be suggested upon observation of the structures of compounds **10**. From comparison of the picture and the hydrogenation results, it can be concluded that catalysts with a Ph or Pr¹ group in the R¹ position lead to the more enantioselective catalysts, while catalyst precursors with a smaller Me group produced lower ee values. Therefore, it is reasonable to assume that hydrogen addition to diastereomer **G** should be made more difficult by a bulky R¹ substituent and consequently the production of the minor *S* enantiomer, thus enhancing the enantioselectivity (Figure 7).³⁴ Note that the more enantioselective catalysts approximately reproduce the arrangement depicted by C₂ symmetric diphosphines, with alternate quadrants offering the larger steric impediment. Therefore, in the case of our ligands, although an excellent enantioselectivity

(31) Reetz, M. T.; Neugebauer, T. *Angew. Chem., Int. Ed. Engl.* **1999**, *38*, 179.

(32) The structure of dihydrides **K** and **K'** has been proposed by similarity with those described in ref 28.

(33) Burk, M. J.; Kalberg, C. S.; Pizzano, A. *J. Am. Chem. Soc.* **1998**, *120*, 4345.

(34) In Figure 7 the positions of R¹ and R² have been assumed for *S* phosphite configuration. Then, the figure would be applicable for an enantiomer of **5f**, in which the Ph group would occupy the position denoted by R¹.

**Figure 6.****Figure 7.**

tivity can be obtained with only a chiral phosphite group, its influence is also extended to the phosphine group, hence, the high enantioselectivity is a consequence of a synergistic action between both coordinating fragments.

Conclusions

A convenient synthesis of new modularly designed chiral phosphine–phosphites, which differ in the nature

of the phosphine group and in the position of the stereogenic element, has been described. An investigation of the electronic properties of the two phosphorus functionalities of compounds **5** indicates substantial differences between them. Thus, studies of $^1J_{\text{PSe}}$ values of the corresponding diselenides in connection with IR analysis of compounds Rh(Cl)(CO)(P–OP) are in accordance with a rather reduced σ -donor ability and a strong π -acceptor character of the phosphite fragment. Moreover, this functionality experiences a variable back-donation from the metal, thus compensating the different basicity of the phosphine fragment along the series of ligands. Overall, these phosphine–phosphites are considerably less donating than diphosphines.

An investigation of the structure of the coordinated phosphine–phosphite indicates a suitable scaffold for asymmetric catalytic hydrogenation due to the arrangement of the phosphite fragment. In addition, interaction between the phosphite and the rather rigid backbone led to a preferred conformation of the latter.

Due to the substantial electronic differences between the coordinating functionalities, MAC prefers to coordinate its olefinic bond *cis* to the phosphite, as evidenced by detailed NMR studies. The proximity between the phosphite and the coordinated olefin causes the former to direct the enantioselectivity of the process. However, the phosphine group exerts a secondary action and, for the attainment of a product of high optical purity, it is necessary to use an adequate phosphine group. Interestingly, this double effect can be accomplished with ligands which are only chiral at the phosphite, thus simplifying the catalyst design, as the influence of the phosphite is extended to the phosphine group.

Experimental Section

General Procedures. All reactions and manipulations were performed under nitrogen or argon, either in a Braun Labmaster 100 glovebox or with standard Schlenk-type techniques. All solvents were distilled under nitrogen with the following desiccants: sodium-benzophenone-ketyl for benzene, diethyl ether (Et₂O,) and tetrahydrofuran (THF); sodium for petroleum ether and toluene; CaH₂ for dichloromethane (CH₂Cl₂); and NaOMe for methanol (MeOH). NMR spectra were obtained on Bruker DPX-300, DRX-400, or DRX-500 spectrometers. $^{31}\text{P}\{^1\text{H}\}$ NMR shifts were referenced to external 85% H₃PO₄, while $^{13}\text{C}\{^1\text{H}\}$ and ^1H shifts were referenced to the residual signals of deuterated solvents. All data are reported in ppm downfield from Me₄Si. GC analyses were performed by using a Hewlett-Packard Model HP 6890 chromatograph. HRMS data were obtained on a JEOL JMS-SX 102A mass spectrometer. Elemental analyses were run by the Analytical Service of the Instituto de Investigaciones Químicas. Optical rotations were measured on a Perkin-Elmer Model 341 polarimeter.

Synthesis of Phosphonium Bromides (2). These compounds were prepared by demethylation of anisyl phosphines **1**, as described below for derivative **2c**.

Diisopropyl-1-(2-hydroxyphenyl)phosphonium Bromide (2c). To a stirred solution of *o*-anisyl-diisopropylphosphine (3.0 g, 13.4 mmol) in CH₂Cl₂ (100 mL) cooled at –78 °C was added BBr₃ (3.0 mL, 31.7 mmol) via syringe. The resulting solution was left to warm to room temperature, stirred for 12 h, and carefully evaporated to dryness. A portion of toluene was added to the residue and then evaporated to secure the evaporation of volatiles. The resulting solid was treated with MeOH (20 mL) at 0 °C and stirred for 48 h at room temperature. Volatiles were evaporated and the resulting oil dissolved

in CH₂Cl₂ and precipitated with Et₂O, yielding a white solid (3.1 g, 80%). ^1H NMR (CDCl₃, 300 MHz): δ 1.20 (dd, $^3J_{\text{HP}} = 19.4$ Hz, $^3J_{\text{HH}} = 7.2$ Hz, 6H, 2 CHMe₂), 1.35 (dd, $^3J_{\text{HP}} = 19.8$ Hz, $^3J_{\text{HH}} = 7.1$ Hz, 6H, 2 CHMe₂), 3.01 (m, 2H, 2 CHMe₂), 6.87 (tdd, $^3J_{\text{HH}} = 7.5$ Hz, $^4J_{\text{HP}} = 2.3$ Hz, $^4J_{\text{HH}} = 1.0$ Hz, 1H, H arom), 7.36 (dt, $^1J_{\text{HP}} = 468$ Hz, $^3J_{\text{HH}} = 7.0$ Hz, 1H, P–H), 7.41 (m, 1H, H arom), 7.58 (ddd, $^3J_{\text{HP}} = 14.8$ Hz, $^3J_{\text{HH}} = 7.6$ Hz, $^4J_{\text{HH}} = 1.3$ Hz, 1H, H arom), 7.73 (m, 1H, H arom), 10.39 (s, 1H, O–H). $^{31}\text{P}\{^1\text{H}\}$ NMR (CDCl₃, 121 MHz): δ 33.1. $^{13}\text{C}\{^1\text{H}\}$ NMR (CDCl₃, 75 MHz): δ 17.7 (d, $J_{\text{CP}} = 2$ Hz, 2 CHMe₂), 18.1 (2 CHMe₂), 21.2 (d, $J_{\text{CP}} = 44$ Hz, 2 CHMe₂), 98.9 (d, $J_{\text{CP}} = 79$ Hz, C_q arom), 118.1 (d, $J_{\text{CP}} = 7$ Hz, CH arom), 121.0 (d, $J_{\text{CP}} = 12$ Hz, CH arom), 135.9 (d, $J_{\text{CP}} = 7$ Hz, CH arom), 137.3 (CH arom), 161.7 (C_q arom). Anal. Calcd for C₁₂H₂₀POBr: C, 49.5; H, 6.9. Found: C, 49.4; H, 6.7.

Preparation of Phenol–Phosphines 3. Compounds **3** were synthesized by deprotonation of phosphonium bromides **2**. Below the preparation of compound **3c** is described.

Diisopropyl-1-(2-hydroxyphenyl)phosphine (3c). Phosphonium salt **2c** (0.69 g, 2.4 mmol) was suspended in toluene (25 mL) and NEt₃ (0.8 mL, 5.5 mmol) added. The resulting mixture was stirred vigorously for 2 h and filtered. Evaporation of the solvent produced a colorless oil (0.50 g, 99%). IR (Nujol mull, cm^{–1}): 3380 (s, $\nu(\text{OH})$). ^1H NMR (CDCl₃, 500 MHz): δ 0.92 (dd, $^3J_{\text{HP}} = 12.4$ Hz, $^3J_{\text{HH}} = 6.9$ Hz, 6H, 2 CHMe₂), 1.11 (dd, $^3J_{\text{HP}} = 16.6$ Hz, $^3J_{\text{HH}} = 7.0$ Hz, 6H, 2 CHMe₂), 2.14 (hd, $^3J_{\text{HH}} = 7.0$ Hz, $^2J_{\text{HP}} = 3.7$ Hz, 2H, 2 CHMe₂), 6.87–6.92 (m, 2H, 2 H arom), 6.98 (br s, 1H, O–H), 7.23–7.26 (m, 2H, 2 H arom). $^{31}\text{P}\{^1\text{H}\}$ NMR (CDCl₃, 202 MHz): δ –25.3. $^{13}\text{C}\{^1\text{H}\}$ NMR (CDCl₃, 126 MHz): δ 18.7 (d, $J_{\text{CP}} = 7$ Hz, 2 CHMe₂), 20.0 (d, $J_{\text{CP}} = 18$ Hz, 2 CHMe₂), 22.9 (d, $J_{\text{CP}} = 6$ Hz, 2 CHMe₂), 114.9 (CH arom), 118.1 (d, $J_{\text{CP}} = 8$ Hz, C_q arom), 119.9 (CH arom), 131.0 (CH arom), 132.6 (CH arom), 161.1 (d, $J_{\text{CP}} = 19$ Hz, C_q arom). HRMS (EI): m/z 211.1247, [M + H]⁺ (exact mass calculated for C₁₂H₂₀OP: 211.1252).

(S)-3,3'-Di-tert-butyl-5,5',6,6'-tetramethyl-2,2'-bisphenoxyphosphorus Chloride ((S)-4a). (S)-3,3'-di-tert-butyl-5,5',6,6'-tetramethyl-2,2'-bisphenol (4.6 g, 13.0 mmol) was azeotropically dried with toluene (2 × 30 mL), dissolved in toluene (100 mL), and added dropwise over a mixture of PCl₃ (1.1 mL, 13.0 mmol) and pyridine (2.3 mL, 28.6 mmol) dissolved in 60 mL of toluene. The resulting suspension was stirred for 14 h, filtered, and evaporated to dryness to yield (S)-**4a** as a white solid (5.0 g, 92%). [α]_D²⁰ 508 (c 1.0, THF). ^1H NMR (CD₂Cl₂, 300 MHz): δ 1.44 (s, 9H, CMe₃), 1.45 (s, 9H, CMe₃), 1.82 (s, 3H, Ar-Me), 1.88 (s, 3H, Ar-Me), 2.29 (s, 3H, Ar-Me), 2.30 (s, 3H, Ar-Me), 7.24 (s, 1H, H arom), 7.27 (s, 1H, H arom). $^{31}\text{P}\{^1\text{H}\}$ NMR (CD₂Cl₂, 121 MHz): δ 163.1. $^{13}\text{C}\{^1\text{H}\}$ NMR (CD₂Cl₂, 75 MHz): δ 16.5 (Ar-Me), 16.8 (Ar-Me), 20.5 (2 Ar-Me), 31.2 (d, $J_{\text{CP}} = 5$ Hz, CMe₃), 32.3 (CMe₃), 34.9 (CMe₃), 35.3 (CMe₃), 128.7 (CH arom), 129.3 (CH arom), 130.6 (C_q arom), 131.9 (d, $J_{\text{CP}} = 6$ Hz, C_q arom), 133.5 (C_q arom), 134.5 (C_q arom), 135.0 (C_q arom), 136.0 (C_q arom), 137.9 (C_q arom), 138.7 (C_q arom), 144.0 (C_q arom), 145.6 (C_q arom). HRMS (EI): m/z 418.1829, [M]⁺ (exact mass calculated for C₂₄H₃₂O₂-PCl: 418.1828).

Synthesis of Phosphine–phosphites (5). Ligands **5** were prepared by condensation between a phenol phosphine (**3**) and an equimolar amount of the appropriate chlorophosphite (**4**) in the presence of NEt₃. A representative procedure is described for **5c**.

Compound 5c. Phosphonium bromide **2c** (0.69 g, 2.3 mmol) was suspended in toluene (25 mL) and NEt₃ (0.8 mL, 5.7 mmol) was added. The resulting suspension was stirred for 2 h and filtered. The solution obtained was evaporated to dryness and subjected to further drying by addition of portions of toluene (2 × 20 mL). The resulting oil was dissolved in toluene (50 mL) and the solution added dropwise over a mixture of (S)-**4a** (0.91 g, 2.3 mmol) and NEt₃ (0.4 mL, 2.8 mmol) dissolved in toluene (60 mL). The reaction was stirred for 48 h and filtered and volatiles were removed, resulting a colorless oil that was

redissolved in Et₂O and passed through a short pad of neutral alumina, yielding compound **5c** as a white foamy solid (1.0 g, 71%). [α]_D²⁰ 347 (c 1.0, THF). ¹H NMR (CD₂Cl₂, 300 MHz): δ 0.79 (dd, ³J_{HP} = 11.2 Hz, ³J_{HH} = 7.0 Hz, 3H, CHMe₂), 0.83 (dd, ³J_{HP} = 13.0 Hz, ³J_{HH} = 7.0 Hz, 3H, CHMe₂), 1.02 (dd, ³J_{HP} = 10.8 Hz, ³J_{HH} = 7.0 Hz, 3H, CHMe₂), 1.07 (dd, ³J_{HP} = 10.9 Hz, ³J_{HH} = 7.0 Hz, 3H, CHMe₂), 1.31 (s, 9H, CMe₃), 1.40 (s, 9H, CMe₃), 1.83 (s, 3H, Ar-Me), 1.88 (s, 3H, Ar-Me), 1.98 (h, ³J_{HH} = 7.0 Hz, 1H, CHMe₂), 1.98 (hd, ³J_{HH} = 7.0 Hz, ²J_{HP} = 1.6 Hz, 1H, CHMe₂), 2.27 (s, 3H, Ar-Me), 2.32 (s, 3H, Ar-Me), 6.60 (m, 1H, H arom), 7.05 (dt, ³J_{HH} = 7.3 Hz, ⁴J_{HH} = 0.9 Hz, 1H, H arom), 7.14 (m, 1H, H arom), 7.16 (s, 1H, H arom), 7.23 (s, 1H, H arom), 7.42 (ddd, ³J_{HH} = 7.1 Hz, ⁴J_{HP} = 4.7 Hz, ⁴J_{HH} = 1.8 Hz, 1H, H arom). ³¹P{¹H} NMR (CD₂Cl₂, 121 MHz): δ -1.0 (br d, P-C), 129.3 (d, ⁴J_{PP} = 32 Hz, P-O). ¹³C{¹H} NMR (CD₂Cl₂, 126 MHz): δ 16.4 (Ar-Me), 16.7 (Ar-Me), 19.7 (d, J_{CP} = 9 Hz, CHMe₂), 20.4 (2 Ar-Me), 20.5 (d, J_{CP} = 21 Hz, CHMe₂), 20.6 (d, J_{CP} = 14 Hz, CHMe₂), 20.7 (d, J_{CP} = 19 Hz, CHMe₂), 23.3 (d, J_{CP} = 12 Hz, CHMe₂), 24.5 (d, J_{CP} = 14 Hz, CHMe₂), 31.2 (d, J_{CP} = 5 Hz, CMe₃), 31.5 (CMe₃), 34.8 (CMe₃), 35.0 (CMe₃), 121.3 (d, J_{CP} = 13 Hz, CH arom), 123.5 (d, J_{CP} = 3 Hz, CH arom), 128.1 (CH arom), 128.3 (C_q arom), 128.5 (CH arom), 129.9 (CH arom), 131.1 (C_q arom), 132.3 (2 C_q arom), 133.1 (C_q arom), 134.7 (C_q arom), 135.3 (d, J_{CP} = 9 Hz, CH arom), 135.4 (C_q arom), 137.8 (C_q arom), 138.6 (C_q arom), 145.0 (C_q arom), 145.4 (d, J_{CP} = 6 Hz, C_q arom), 156.1 (d, J_{CP} = 14 Hz, C_q arom). HRMS (ED): *m/z* 592.3240, [M]⁺ (exact mass calculated for C₃₆H₅₀O₃P₂: 592.3235).

Diselenides 7. Derivatives **7** were prepared by heating a solution in toluene of the corresponding phosphine–phosphite in contact with elemental selenium as described below for **7c**.

Compound 7c. Over a solution of **5c** (0.020 g, 0.03 mmol) in toluene (0.5 mL) was added elemental selenium (0.011 g, 0.14 mmol) and the mixture was heated at 100 °C for 8 days. The resulting mixture was filtered through Celite and evaporated to dryness, resulting an oil that was additionally dried by adding a portion of benzene. Evaporation of volatiles rendered compound **7c** quantitatively as a white solid. [α]_D²⁰ 162 (c 1.0, THF). ¹H NMR (CDCl₃, 500 MHz): δ 0.59 (dd, ³J_{HP} = 19.2 Hz, ³J_{HH} = 6.9 Hz, 3H, CHMe₂), 0.74 (dd, ³J_{HP} = 19.3 Hz, ³J_{HH} = 6.9 Hz, 3H, CHMe₂), 1.06 (dd, ³J_{HP} = 18.5 Hz, ³J_{HH} = 6.7 Hz, 3H, CHMe₂), 1.20 (dd, ³J_{HP} = 18.7 Hz, ³J_{HH} = 6.7 Hz, 3H, CHMe₂), 1.31 (s, 9H, CMe₃), 1.43 (s, 9H, CMe₃), 1.79 (s, 3H, Ar-Me), 1.90 (s, 3H, Ar-Me), 2.26 (s, 3H, Ar-Me), 2.32 (s, 3H, Ar-Me), 2.55 (dh, ²J_{HP} = 6.5 Hz, ³J_{HH} = 6.5 Hz, 1H, CHMe₂), 3.11 (dh, ²J_{HP} = 6.7 Hz, ³J_{HH} = 6.7 Hz, 1H, CHMe₂), 6.84 (br s, 1H, H arom), 7.18 (s, 1H, H arom), 7.21 (m, 2H, 2 H arom), 7.27 (s, 1H, H arom), 8.47 (m, 1H, H arom). ³¹P{¹H} NMR (CDCl₃, 202 MHz): δ 52.7 (¹J_{PSe} = 1053 Hz, P-O), 75.7 (¹J_{PSe} = 719 Hz, P-C). ¹³C{¹H} NMR (CDCl₃, 126 MHz): δ 16.5 (Ar-Me), 16.6 (Ar-Me), 18.4 (CHMe₂), 18.6 (CHMe₂), 18.8 (CHMe₂), 19.0 (CHMe₂), 20.4 (Ar-Me), 20.5 (Ar-Me), 26.7 (d, J_{CP} = 43 Hz, CHMe₂), 27.7 (d, J_{CP} = 43 Hz, CHMe₂), 31.1 (CMe₃), 32.9 (CMe₃), 34.8 (CMe₃), 35.4 (CMe₃), 119.7 (dd, J_{CP} = 56, 9 Hz, C_q arom), 119.9 (CH arom), 124.9 (d, J_{CP} = 11 Hz, CH arom), 129.0 (C_q arom), 129.1 (CH arom), 129.5 (C_q arom), 130.7 (CH arom), 132.5 (CH arom), 134.0 (C_q arom), 134.6 (C_q arom), 135.6 (2 C_q arom), 137.6 (d, J_{CP} = 4 Hz, C_q arom), 138.2 (d, J_{CP} = 5 Hz, C_q arom), 139.9 (d, J_{CP} = 10 Hz, CH arom), 143.1 (d, J_{CP} = 9 Hz, C_q arom), 145.8 (d, J_{CP} = 16 Hz, C_q arom), 151.3 (d, J_{CP} = 12 Hz, C_q arom). HRMS (FAB): *m/z* 753.1646, [M + H]⁺ (exact mass calculated for C₃₆H₅₁O₃P₂Se₂: 753.1644).

RhCl(CO)(P-OP) Complexes (8). Chlorocarbonyls were prepared by reacting [RhCl(C₂H₄)₂]₂ with the appropriate phosphine–phosphite followed by treatment of the resulting mixture with carbon monoxide. Below is described a representative preparation.

RhCl(CO)(5c) (8c). A solution of **5c** (0.107 g, 0.18 mmol) in THF (5 mL) was added slowly over a stirred solution of [Rh-(*u*-Cl)(C₂H₄)₂]₂ (0.035 g, 0.09 mmol) in THF (5 mL). The

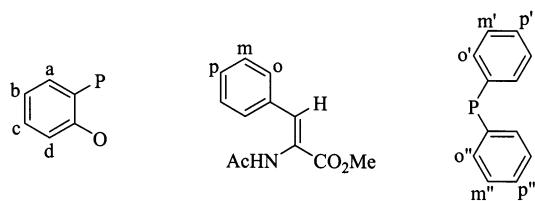
mixture was stirred for 30 min, and then CO was bubbled through the mixture for 15 min, changing the color of the solution from orange to yellow. The mixture was evaporated to dryness and the resulting solid was recrystallized from a mixture of hexanes/Et₂O (3:1) giving **8c** as a yellow powder (0.086 g, 63%). Attempts to obtain satisfactory elemental analysis for this compound have proven fruitless. IR (Nujol mull, cm⁻¹): 2042 (s, ν (CO)). ¹H NMR (CD₂Cl₂, 400 MHz): δ 1.16 (dd, ³J_{HP} = 14.3 Hz, ³J_{HH} = 7.0 Hz, 3H, CHMe₂), 1.30 (dd, ³J_{HP} = 16.8 Hz, ³J_{HH} = 7.2 Hz, 3H, CHMe₂), 1.34 (dd, ³J_{HP} = 16.3 Hz, ³J_{HH} = 7.2 Hz, 3H, CHMe₂), 1.37 (s, 9H, CMe₃), 1.46 (s, 9H, CMe₃), 1.54 (dd, ³J_{HP} = 15.8 Hz, ³J_{HH} = 7.1 Hz, 3H, CHMe₂), 1.83 (s, 6H, 2 Ar-Me), 2.26 (s, 3H, Ar-Me), 2.31 (s, 3H, Ar-Me), 2.64 (dh, ³J_{HP} = 7.0 Hz, ²J_{HP} = 7.0 Hz, 1H, CHMe₂), 3.06 (dh, ²J_{HP} = 12.8 Hz, ³J_{HH} = 7.0 Hz, 1H, CHMe₂), 6.74 (ddt, ³J_{HH} = 7.1 Hz, ⁴J_{HP} = 4.3 Hz, ⁴J_{HH} = 1.0 Hz, 1H, H arom), 7.23 (s, 1H, H arom), 7.25 (m, 1H, H arom), 7.27 (s, 1H, H arom), 7.41 (t, ³J_{HH} = 7.4 Hz, 1H, H arom), 7.56 (ddd, ³J_{HP} = 7.9 Hz, ³J_{HH} = 6.5 Hz, ⁴J_{HH} = 1.6 Hz, 1H, H arom). ³¹P{¹H} NMR (CD₂Cl₂, 162 MHz): δ 16.2 (dd, ¹J_{PRh} = 122 Hz, P-C), 133.5 (dd, ¹J_{PRh} = 278 Hz, ²J_{PP} = 62 Hz, P-O). ¹³C{¹H} NMR (CD₂Cl₂, 126 MHz): δ 16.5 (Ar-Me), 16.6 (Ar-Me), 18.3 (CHMe₂), 19.1 (d, J_{CP} = 3 Hz, CHMe₂), 19.5 (CHMe₂), 20.2 (Ar-Me), 20.4 (Ar-Me), 20.6 (d, J_{CP} = 4 Hz, CHMe₂), 24.1 (d, J_{CP} = 24 Hz, CHMe₂), 27.3 (d, J_{CP} = 23 Hz, CHMe₂), 31.6 (CMe₃), 32.9 (CMe₃), 35.1 (CMe₃), 35.5 (CMe₃), 115.6 (dd, J_{CP} = 35, 10 Hz, C_q arom), 122.7 (CH arom), 125.0 (d, J_{CP} = 4 Hz, CH arom), 128.8 (CH arom), 129.5 (CH arom), 130.0 (d, J_{CP} = 2 Hz, C_q arom), 130.7 (C_q arom), 131.9 (CH arom), 132.8 (CH arom), 133.3 (C_q arom), 134.0 (C_q arom), 135.1 (C_q arom), 135.9 (C_q arom), 137.6 (C_q arom), 138.2 (d, J_{CP} = 4 Hz, C_q arom), 143.6 (d, J_{CP} = 7 Hz, C_q arom), 146.3 (d, J_{CP} = 14 Hz, C_q arom), 156.3 (d, J_{CP} = 10, 3 Hz, C_q arom), 182.9 (ddd, J_{CP} = 110, 13 Hz, J_{CRh} = 63 Hz, CO).

[(COD)Rh(P-OP)]BF₄ Complexes (9). Compounds **9** were prepared by reaction of [(COD)₂Rh]BF₄ with a stoichiometric amount of the appropriate phosphine–phosphite as described for **9c**.

[(COD)Rh(5c)]BF₄ (9c). Over a stirred solution of [(COD)₂Rh]BF₄ (0.100 g, 0.25 mmol) in CH₂Cl₂ (5 mL) was added slowly **5c** (0.153 g, 0.26 mmol) dissolved in CH₂Cl₂ (10 mL). The resulting orange solution was stirred for 20 min, and then concentrated to a fourth of the volume. The mixture was filtered and precipitated with Et₂O (45 mL). The resulting solid was washed with Et₂O (2 × 10 mL) and recrystallized from a mixture of CH₂Cl₂/Et₂O (1:3), yielding **9c** as an orange-yellow solid (0.152 g, 68%). ¹H NMR (CD₂Cl₂, 500 MHz): δ 0.99 (dd, ³J_{HP} = 13.4 Hz, ³J_{HH} = 6.8 Hz, 3H, CHMe₂), 1.24 (s, 9H, CMe₃), 1.30 (dd, ³J_{HP} = 17.3 Hz, ³J_{HH} = 6.8 Hz, 3H, CHMe₂), 1.38 (dd, ³J_{HP} = 14.6 Hz, ³J_{HH} = 6.7 Hz, 3H, CHMe₂), 1.50 (s, 9H, CMe₃), 1.58 (dd, ³J_{HP} = 18.2 Hz, ³J_{HH} = 7.1 Hz, 3H, CHMe₂), 1.76 (s, 3H, Ar-Me), 1.84 (s, 3H, Ar-Me), 2.11–2.65 (m, 9H, 4 CH₂ COD and CHMe₂), 2.30 (s, 3H, Ar-Me), 2.32 (s, 3H, Ar-Me), 3.08 (h, ³J_{HH} = 7.1 Hz, 1H, CHMe₂), 3.93 (br m, 1H, =CH COD), 5.65 (br m, 1H, =CH COD), 5.90 (br m, 1H, =CH COD), 6.19 (br m, 1H, =CH COD), 6.70 (m, 1H, H arom), 7.24 (s, 1H, H arom), 7.33 (s, 1H, H arom), 7.38 (m, 1H, H arom), 7.47 (m, 2H, 2 H arom). ³¹P{¹H} NMR (CD₂Cl₂, 202 MHz): δ 14.9 (dd, ¹J_{PRh} = 137 Hz, P-C), 129.7 (dd, ¹J_{PRh} = 265 Hz, ²J_{PP} = 45 Hz, P-O). ¹³C{¹H} NMR (CD₂Cl₂, 126 MHz): δ 16.4 (Ar-Me), 16.6 (Ar-Me), 17.4 (d, J_{CP} = 2 Hz, CHMe₂), 17.6 (d, J_{CP} = 5 Hz, CHMe₂), 19.7 (d, J_{CP} = 4 Hz, CHMe₂), 20.2 (Ar-Me), 20.4 (Ar-Me), 22.5 (d, J_{CP} = 4 Hz, CHMe₂), 23.9 (d, J_{CP} = 22 Hz, CHMe₂), 28.8 (CH₂ COD), 29.2 (CH₂ COD), 29.9 (d, J_{CP} = 23 Hz, CHMe₂), 31.8 (CMe₃ and CH₂ COD), 32.1 (CH₂ COD), 32.3 (CMe₃), 35.0 (CMe₃), 35.2 (CMe₃), 91.3 (dd, J_{CP} = 9 Hz, J_{CRh} = 7 Hz, =CH COD), 103.1 (t, J_{CP} = 7 Hz, J_{CRh} = 7 Hz, =CH COD), 106.6 (dd, J_{CP} = 11 Hz, J_{CRh} = 5 Hz, =CH COD), 108.6 (dd, J_{CP} = 14 Hz, J_{CRh} = 5 Hz, =CH COD), 114.5 (dd, J_{CP} = 36, 10 Hz, C_q arom), 123.6 (CH arom), 126.4 (d, J_{CP} = 3 Hz, CH arom), 129.0 (CH arom), 129.2 (C_q arom), 129.6 (CH

arom and C_q arom), 131.7 (CH arom), 133.6 (CH arom), 134.5 (C_q arom), 134.7 (C_q arom), 135.7 (C_q arom), 136.6 (C_q arom), 137.5 (2 C_q arom), 144.0 (d, J_{CP} = 7 Hz, C_q arom), 144.7 (d, J_{CP} = 14 Hz, C_q arom), 155.1 (dd, J_{CP} = 8, 5 Hz, C_q arom). Anal. Calcd for C₄₄H₆₂O₃BF₄P₂Rh·0.5CH₂Cl₂: C, 57.3; H, 6.8. Found: C, 57.4; H, 6.7.

[Rh(5a)(MAC)]BF₄ (10a). **10a** was obtained as an orange solid as described for **10c**. ¹H NMR (CD₂Cl₂, 500 MHz): δ 1.25 (s, 9H, CMe₃), 1.42 (s, 9H, CMe₃), 1.82 (s, 3H, Ar-Me), 1.87 (s, 3H, Ar-Me), 2.06 (s, 3H, C(O)Me), 2.27 (s, 3H, Ar-Me), 2.37 (s, 3H, Ar-Me), 3.05 (s, 3H, OMe), 6.55 (dd, ³J_{HH} = 7.8 Hz, ⁴J_{HP} = 5.6 Hz, 1H, H^d), 6.72 (ddd, ³J_{HP} = 9.4 Hz, ³J_{HH} = 8.0 Hz, ⁴J_{HH} = 1.4 Hz, 1H, H^a), 6.81 (dd, ³J_{HP} = 12.8 Hz, ³J_{HH} = 7.5 Hz, 2H, 2 H^o), 7.10 (m, 3H, 2 H^m and C=CH), 7.14 (m, 1H, H^b), 7.19 (s, 1H, H arom), 7.25 (m, 4H, 2 H^m and 2 H^o), 7.32 (s, 1H, H arom), 7.40 (m, 1H, H^p), 7.53 (m, 6H, H^c, H^p, 2 H^o and 2 H^m), 7.64 (m, 1H, H^p), 8.90 (br s, 1H, NH). ³¹P{¹H} NMR (CD₂Cl₂, 121 MHz): δ 6.0 (dd, ¹J_{PRh} = 152 Hz, P-C), 134.3 (dd, ¹J_{PRh} = 263 Hz, ²J_{PP} = 69 Hz, P-O). ¹³C{¹H} NMR (CD₂Cl₂, 75 MHz): δ 16.7 (2 Ar-Me), 20.2 (d, J_{CRh} = 5 Hz, C(O)Me), 20.4 (Ar-Me), 20.5 (Ar-Me), 31.3 (CMe₃), 31.7 (CMe₃), 34.8 (CMe₃), 35.2 (CMe₃), 52.4 (OMe), 85.8 (d, J_{CP} = 11 Hz, C=CH), 87.4 (dd, J_{CP} = 21 Hz, J_{CRh} = 7 Hz, C=CH), 115.7 (dd, J_{CP} = 55, 8 Hz, C_q arom), 122.3 (CH arom), 126.1 (d, J_{CP} = 7 Hz, CH arom), 127.5 (d, J_{CP} = 54 Hz, C_q), 127.9 (d, J_{CP} = 49 Hz, C_q), 128.7 (2 CH arom), 128.8 (2 CH arom), 129.0 (CH arom), 129.3 (2 CH arom), 129.4 (2 CH arom), 129.4 (2 CH arom), 129.5 (2 CH arom), 129.8 (C_q arom), 129.9 (2 CH arom), 131.4 (C_q arom), 132.0 (C_q arom), 133.2 (C_q arom), 133.7 (CH arom), 133.8 (CH arom), 133.9 (2 CH arom), 134.2 (C_q arom), 134.3 (C_q arom), 136.1 (C_q arom), 136.3 (C_q arom), 137.2 (C_q arom), 145.2 (d, J_{CP} = 8 Hz, C_q arom), 146.1 (d, J_{CP} = 13 Hz, C_q arom), 155.3 (dd, J_{CP} = 10, 2 Hz, C_q arom), 165.8 (d, J_{CP} = 5 Hz, C(O)Me), 184.6 (br s, CO₂Me).

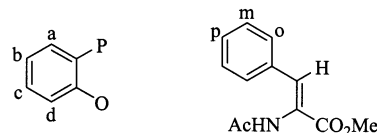


[Rh(5c)(MAC)]BF₄ (10c). A solution of [(COD)Rh(5c)]BF₄ (0.045 g, 0.05 mmol) and norbornadiene (0.50 g, 5.4 mmol) in CH₂Cl₂ (3 mL) was stirred overnight. The resulting mixture was evaporated under reduced pressure and the residue washed with Et₂O (2 × 5 mL) and redissolved in CH₂Cl₂, and the resulting solution was filtered through Celite. The obtained solution was evaporated and dissolved in DME (5 mL), and the solution was hydrogenated in a Fischer–Porter reaction vessel under 4 atm for 5 h. To the resulting solution was added MAC (0.011 g, 0.05 mmol) and the mixture obtained was stirred overnight. The solution was evaporated to dryness and the resulting solid washed with petroleum ether, dissolved in CH₂Cl₂, and filtered through Celite. Evaporation of the solvent produced compound **10c** as an orange powder. ¹H NMR (CD₂Cl₂, 500 MHz): δ 0.63 (dd, ³J_{HP} = 18.5 Hz, ³J_{HH} = 7.0 Hz, 3H, CHMe₂), 0.78 (dd, ³J_{HP} = 15.0 Hz, ³J_{HH} = 6.9 Hz, 3H, CHMe₂), 1.29 (s, 9H, CMe₃), 1.32 (dd, ³J_{HP} = 17.8 Hz, ³J_{HH} = 7.2 Hz, 3H, CHMe₂), 1.49 (dd, ³J_{HH} = 7.1 Hz, 3H, CHMe₂), 1.51 (s, 9H, CMe₃), 1.82 (s, 6H, 2 Ar-Me), 2.03 (br m, 1H, CHMe₂), 2.25 (s, 3H, Ar-Me), 2.30 (s, 3H, C(O)Me), 2.35 (s, 3H, Ar-Me), 2.89 (br m, 1H, CHMe₂), 3.01 (s, 3H, OMe), 6.20 (dd, ³J_{HH} = 8.0 Hz, ⁴J_{HP} = 4.4 Hz, 1H, H^a), 6.77 (dd, ³J_{HP} = 4.8 Hz, ²J_{HRh} = 2.8 Hz, 1H, C=CH), 7.16 (s, 1H, H arom), 7.27 (m, 1H, H^c), 7.30 (s, 1H, H arom), 7.34–7.40 (m, 3H, H^b and 2 H^m), 7.44–7.49 (m, 4H, H^a, 2 H^o and H^p), 8.62 (br s, 1H, NH). ³¹P{¹H} NMR (CD₂Cl₂, 121 MHz): δ 19.2 (dd, ¹J_{PRh} = 151 Hz, P-C), 136.6 (dd, ¹J_{PRh} = 259 Hz, ²J_{PP} = 63 Hz, P-O). ¹³C{¹H} NMR (CD₂Cl₂, 75 MHz): δ 16.6 (Ar-Me), 16.7 (Ar-Me), 16.8 (d, J_{CP}

Table 4. Crystal Data and Data Collection Parameters for **8a**

empirical formula	C ₄₇ H ₅₆ ClO ₅ P ₂ Rh
fw	901.22
temp	299(2) K
wavelength (Mo Kα)	0.71073 Å
cryst syst	orthorhombic
space group	P2(1)2(1)2(1)
unit cell dimens	a = 10.0304(2) Å b = 13.3552(3) Å c = 34.9411(9) Å α = β = γ = 90°
vol	4680.6(2) Å ³
Z	4
calcd density	1.279 g cm ⁻³
abs coeff	0.532 mm ⁻¹
F(000)	1880
cryst size	0.22 × 0.35 × 0.35 mm ³
θ range	1.17 < θ < 23.29°
no. of rflns (collected/unique)	24482/6735
R(int)	0.0485
abs corr	empirical
no. of data/restraints/params	6735/0/517
Goof on F ²	1.035
R[I > 2σ(I)]	R1 = 0.0336
	wR2 = 0.0738
largest diff. peak and hole	0.392/−0.310 e Å ⁻³

= 4 Hz, CHMe₂), 17.5 (d, J_{CP} = 2 Hz, CHMe₂), 19.3 (d, J_{CP} = 3 Hz, CHMe₂), 19.4 (d, J_{CP} = 3 Hz, CHMe₂), 20.1 (d, J_{CRh} = 5 Hz, C(O)Me), 20.4 (Ar-Me), 20.5 (Ar-Me), 23.5 (d, J_{CP} = 24 Hz, CHMe₂), 29.4 (d, J_{CP} = 24 Hz, CHMe₂), 31.7 (CMe₃), 32.0 (CMe₃), 35.0 (CMe₃), 35.3 (CMe₃), 52.3 (OMe), 82.7 (d, J_{CP} = 13 Hz, C=CH), 84.8 (dd, J_{CP} = 23 Hz, J_{CRh} = 8 Hz, C=CH), 114.1 (dd, J_{CP} = 38, 6 Hz, C_q arom), 122.5 (CH arom), 125.8 (d, J_{CP} = 5 Hz, CH arom), 128.6 (CH arom), 129.0 (CH arom), 129.5 (CH arom), 129.5 (2 CH arom), 129.6 (2 CH arom), 130.0 (C_q arom), 131.2 (CH arom), 132.0 (C_q arom), 133.6 (CH arom), 133.9 (C_q arom), 134.2 (C_q arom), 136.0 (C_q arom), 136.4 (d, J_{CP} = 4 Hz, C_q arom), 136.6 (C_q arom), 137.2 (C_q arom), 137.6 (d, J_{CP} = 2 Hz, C_q arom), 145.5 (d, J_{CP} = 9 Hz, C_q arom), 146.0 (d, J_{CP} = 14 Hz, C_q arom), 155.8 (t, J_{CP} = 8 Hz, C_q arom), 166.2 (d, J_{CP} = 5 Hz, C(O)Me), 185.8 (dd, J_{CRh} = 7, J_{CP} = 5 Hz, CO₂-Me).



General Procedure for the Enantioselective Hydrogenations. In a glovebox, a Fischer–Porter reactor (80 mL) was charged with a solution of methyl Z-α-acetamido-cinnamate (MAC) (0.23 g, 1.1 mmol) and **6a** (0.002 g, 0.0022 mmol) in CH₂Cl₂ (5 mL). The vessel was brought outside the glovebox, submitted to vacuum–hydrogen cycles, and finally pressurized to 4 atm. The reaction mixture was stirred for 16 h, then the reactor was depressurized and the mixture obtained was evaporated to dryness, redissolved in an ethyl acetate–hexanes (1:1) mixture, and passed through a short pad of silica. The resulting residue was analyzed by ¹H NMR to determine conversion and by chiral GC for enantiomeric excess as follows: N-acetyl phenylalanine methyl ester (Chrompack Chirasil L-Val, 80 °C (3 min), then 3 °C/min up to 190 °C, 15.0 psi He) (R) t₁ = 32.14 min, (S) t₂ = 32.76 min.

X-ray Structure Determination. Single crystals of **8a** were grown from diethyl ether solution at −30°C. X-ray data were collected on a Bruker SMART 5000 CCD-based diffractometer, using ω-scans and a rotating anode with Mo Kα radiation (λ = 0.71073 Å).³⁵ The frames were integrated with

(35) BrukerAXS, SMART, Area Detector Control Software; Bruker Analytical X-ray Systems: Madison, WI, 1995.

the SAINT software package,³⁶ using a narrow-frame algorithm, and the structure was solved by direct methods, completed by subsequent difference Fourier synthesis, and refined by full-matrix least-squares procedures with SHELXTL 5.1.³⁷ The structure was checked with PLATON.³⁸ Non-H atoms were refined with anisotropic thermal parameters. Hydrogen atoms were treated as idealized contributions. Pertinent crystallographic data are collected in Table 4.

(36) BrukerAXS, *SAINTE*; Integration Software; Bruker Analytical X-ray Systems: Madison, WI, 1995.

(37) Sheldrick, G. M. *SHELXTL* 5.1, Program for Structure Solution and Least Squares Refinement; University of Göttingen: Göttingen, Germany, 1998.

(38) Spek, A. L. *Acta Crystallogr.* **1990**, *A46*, C34. Spek, A. L. *PLATON*, A Multipurpose Crystallographic Tool; Utrecht University: Utrecht, The Netherlands, 2001.

Acknowledgment. We thank Drs. M. L. Poveda, N. Khiar, M. Davies, M. Paneque, and V. Salazar and Prof. E. Carmona for helpful comments. We acknowledge financial support from Ministerio de Ciencia y Tecnología (Grant No. BQU2000-1169). M.A.M-R. also thanks CONACYT-México and Universidad Autónoma del Estado de Hidalgo for a Cátedra de Consolidación Institucional (No. 010316, CIQ-UAEH).

Supporting Information Available: Full experimental and characterization details for the compounds described and representative NMR spectra and crystallographic information for compound **8a**. This material is available free of charge via the Internet at <http://pubs.acs.org>.

OM020140C